Journal of Electrical Systems and Information Technology 3 (2016) 119–126
www.elsevier.com/locate/jesit

Fault ride-through enhancement of fixed speed wind turbine using bridge-type fault current limiter

Mostafa I. Marei *, Hamdy S.K. El-Goharey, Randa M. Toukhy

Electrical Power and Machines Department, Faculty of Engineering, Ain Shams University, Cairo 11517, Egypt

Received 9 July 2015; received in revised form 25 October 2015; accepted 3 January 2016
Available online 17 March 2016

Abstract

The interaction between wind energy turbines and the grid results in two main problems, increasing the short-circuit level and reducing the Fault Ride-Through (FRT) capability during faults. The objective of this paper is to solve these problems, for fixed speed Wind Energy Systems (WECS), utilizing the bridge-type Fault Current Limiter (FCL) with a discharging resistor. A simple cascaded control system is proposed for the FCL to regulate the terminal voltage of the generator and limit the current. The system is simulated on PSCAD/EMTDC software to evaluate the dynamic performance of the proposed WECS compensated by FCL. The simulation results show the potentials of the FCL as a simple and effective method for solving grid interconnection problems of WECS.

Keywords: Fault current limiter (FCL); Fault ride-through (FRT); Voltage regulation; Wind energy conversion systems

1. Introduction

Year after year, the world fossil fuel reserve decreases and clean renewable energy resources are being enormously installed around the world. Wind energy is one of these resources that is widely mounted worldwide due to its reliability and cost effectiveness. The interconnection of the wind farms to the electricity grid may cause stability problems. Moreover, reducing the short circuit current and increasing FRT capability of wind farms are the most important issues. Several solution techniques are investigated in the literature (Firouzi and Gharehpetian, 2013).

Traditionally, the WECS are classified to two main types, namely fixed speed and variable speed. Recently, variable speed wind turbines are mostly used due to their efficiency, improved power quality, and independent control of active and reactive power (Ali, 2012). However, fixed speed WECS were vastly installed over the past-years worldwide, representing a large installed capacity. Since directly connected squirrel cage induction generators, used with fixed

* Corresponding author. Tel.: +2 0100 6957052.
E-mail address: mostafa_ibrahim@eng.asu.edu.eg (M.I. Marei).
Peer review under responsibility of Electronics Research Institute (ERI).

ELSEVIER Production and hosting by Elsevier

http://dx.doi.org/10.1016/j.jesit.2016.01.002
2314-7172/

speed wind turbines, have a lifetime over twenty years, it is essential to study and ameliorate their performance (Ali and Wu, 2010).

Many techniques are proposed to improve the FRT of wind farms such as the pitch control, the shunt, and series compensation. The shunt compensation based techniques include STATic synchronous COMpensator (STATCOM) (Awad et al., 2014; Molinas et al., 2008), Static Var Compensator (SVC) (Molinas et al., 2008), and Thyristor Switched Capacitor (TSC) (Ren et al., 2012). The series compensation based techniques incorporate Dynamic Voltage Restorer (DVR) (Ramirez et al., 2011; Leon et al., 2011), Series Dynamic Braking Resistor (SDBR) (Causebrook et al., 2007), Magnetic Energy Recovery Switch (MERS) (Wiik et al., 2009a), and FCL. Although the pitch control offers the lowest cost solution to improve the LVRT, its dynamic response is low (Rashid and Ali, 2014). The STATCOM and SVC have the capability to enhance the transient stability margin by controlling the reactive power after fault occurrence, however, the mechanical stress increases (Ramirez et al., 2011). The TSC generates no harmonics but the reactive power cannot be varied continuously (Tayyebifar et al., 2014). The DVR is a good solution to improve power quality and isolate the grid faults from the WECS on the account of its bulk size and complex control (Hussein and Ali, 2014). The SDBR has a high reliability, enhances transient stability and needs low maintenance. The main disadvantage of the SDBR is that it allows a sudden rise of fault current instantaneously (Rashid and Ali, 2014; Causebrook et al., 2007). To reduce the switching losses, the MERS is proposed which has a compact size, however, it injects harmonics (Wiik et al., 2009b). The FCL offers an effective and simple solution to enhance the FRT of a WECS. In addition, the FCL is compact in size and limits the instantaneous rise of fault current (Rashid and Ali, 2014; Chen et al., 2013).

This paper presents a simple control system for the bridge-type FCL with a discharging resistor to enhance the FRT capability of a fixed speed WECS.

2. Fault current limiters

There are many types of the FCLs which can be summarized as follows:

1. Superconducting FCL depends on utilizing a superconducting element that has low impedance during normal operation and high impedance when the current rises suddenly. Cooling equipment is needed to control the temperature of the superconducting element for proper operation which increases the cost of this type of FCL (Sheng et al., 2012; de Sousa et al., 2012).
2. Solid-state FCL is based on semiconductor devices which are controlled to inject certain impedance in series with the feeder to limit the fault current. Although this type of FCL is easy to control, it experiences many technical challenges (Abramovitz and Smedley, 2012; Corzine and Ashton, 2012).
3. Saturable core FCL where a dc current saturates the iron core which isolates the secondary side impedance, during normal operation. During faults, the high ac current drives the core out of saturation, inserting the secondary side impedance to the power line. This technology needs bulky devices due to the need for many iron cores (Chen et al., 2013; Cvoric et al., 2009; Abbott et al., 2006).

3. Bridge-type fault current limiter

The non-superconducting bridge-type FCL has been proposed because of its simple control and reduced cost compared to the other types (Hagh and Abapour, 2009; Min et al., 2008). It consists of a diode bridge and a dc reactor L_d as shown in Fig. 1 (Ise et al., 2001). In addition, a resistor in parallel with a semiconductor switch is connected in series with the dc reactor to control the level of the fault current by controlling the dc reactor current.

The FCL is connected between the WECS and the grid through open secondary windings of an insertion transformer where the primary windings are star connected to the bridge-type FCL. During normal operation, the semiconductor switch is turned-on to bypass the discharging resistor. Hence, the impedance seen from open-winding side of the transformer is the smallest and is governed by the equivalent impedance of the transformer. As a result, the dc reactor current i_d is proportional to the generated current from the WECS and within normal values. During grid fault, the dc current value rises suddenly above its limit value. Once the fault is detected, the control circuit turns-off the semiconductor switch to insert the discharging resistor into the feeder between the WECS and the grid. By controlling the switching times of the semiconductor switch, the current level of the wind generator is controlled to be within the limit values (Firouzi and Gharehpetian, 2013).

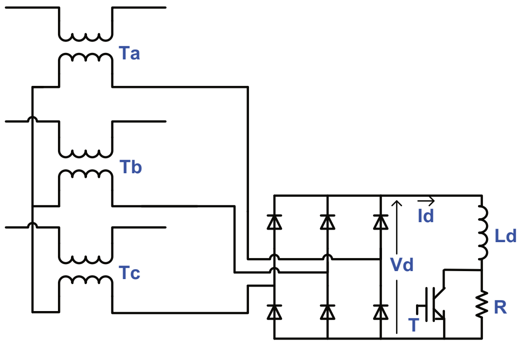

Fig. 1. Bridge-type fault current limiter with a discharging resistor.

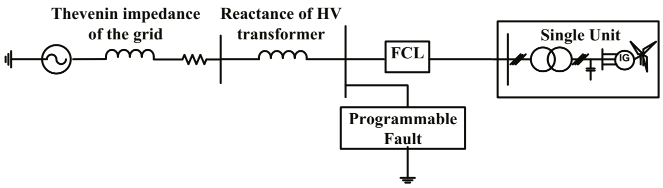

Fig. 2. Fixed speed wind turbine system with FCL.

Fig. 2 shows a fixed speed WECS connected to the grid. The grid is represented by its Thevenin equivalent voltage and impedance. The wind turbine is equipped with a squirrel-cage induction generator, a power factor correction capacitor bank, a step-up transformer and a connection cable. A FCL is connected in between the wind turbine and the low-tension side of the HV transformer at the Point of Common Coupling (PCC), to limit the share of WECS during the grid fault (Marei and El-Goharey, 2013).

4. The proposed control system for the FCL

When a fault occurs, the line current exceeds the rated current and it is transferred to the secondary circuit of the FCL with the turns-ratio of the insertion transformer. The control circuit measures the dc reactor current and utilizes it in the proposed control system. When this current exceeds a predetermined value, a fault condition is detected and the FCL is activated by switching of the semiconductor. The discharging resistor is introduced in the circuit to limit the current and to absorb the energy stored in the dc reactor. The dc reactor current level is hence controlled by controlling the on and off durations of the semiconductor switch (Firouzi and Gharehpetian, 2013). Fig. 3 presents the block diagram of the proposed control system of the FCL to isolate the WECS from the grid fault. It is based on two cascaded loops. The outer loop controls the terminal voltage of the generator, while the inner loop regulates the current. The terminal voltage of the generator V_g is compared to a reference value V_g^* and the error is fed to a simple Proportional Integral (PI) controller. The action of this control loop is the reference signal of the dc reactor current i_d^*. A limiter is utilized to prevent overloading the line connecting the WECS with the PCC. The inner loop utilizes the Hysteresis Current Controller (HCC) to regulate the reactor current i_d at its reference signal by controlling the semiconductor gate signal G.

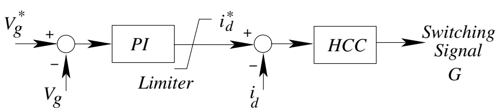

Fig. 3. Block diagram of the proposed FCL control system.

Table 1
System parameters.

Induction generator rating	600 kW, 50 Hz, 4 poles
Step-up transformer	1.05 MVA, 690 V/22 kV
Connection cable	6 mH and 0.8 Ω
Thevenin equivalent of the grid referred to 22 kV	0.2465 mH and 0.00968 Ω
Reactance of the HV transformer	5.83 mH
DC reactor (Ld)	10 mH
Discharging resistor (R)	20 Ω

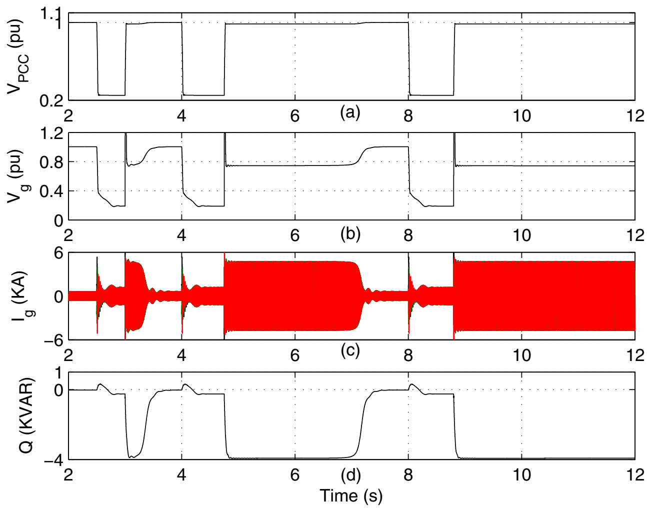

Fig. 4. Dynamic performance under faults without compensation: (a) the PCC rms voltage, (b) the generator rms voltage, (c) the three-phase generator currents, and (d) the reactive power at the generator terminals.

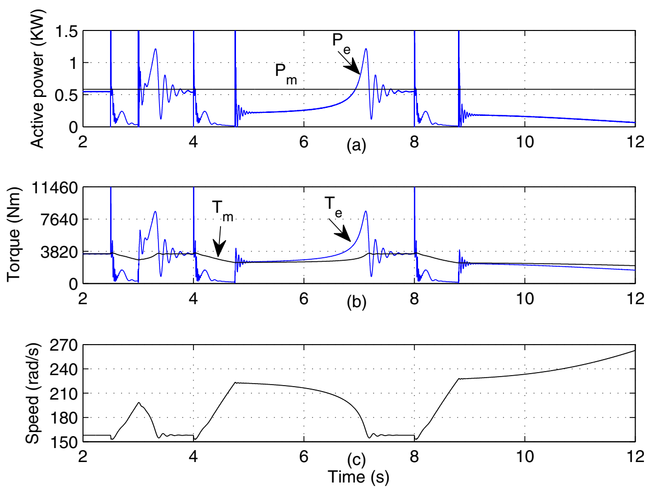

Fig. 5. Dynamic performance under faults without compensation: (a) the turbine and generator powers, (b) the turbine and generator torques, and (c) the generator speed.

5. Simulation results

The system shown in Fig. 2 is represented on PSCAD/EMTDC software package. The parameters of the system are specified in Table 1. The wind speed is assumed to be constant at 13 m/s. As a result, the wind turbine is operated almost at rated power to examine the capability of the proposed FCL at such extreme condition. Two case studies are

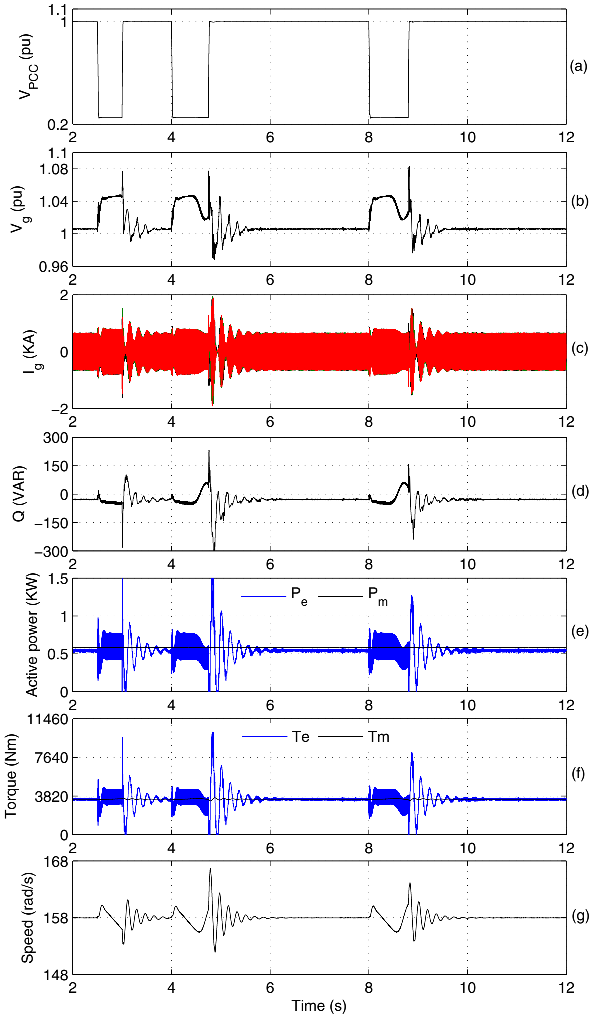

Fig. 6. Dynamic performance under faults with the proposed FCL: (a) the PCC rms voltage, (b) the generator rms voltage, (c) the three-phase generator currents, (d) the reactive power at the generator terminals, (e) the turbine and generator powers, (f) the turbine and generator torques, and (g) the generator speed.

carried out, where different faults with different durations are programmed. The first case illustrates the performance of the WECS without compensation when subjected to three voltage dips with different durations. The second test case is dedicated to examine the system performance when the proposed FCL is applied under the same fault conditions of the first case.

5.1. Fixed speed wind turbine without FCL

Fig. 4 illustrates the dynamic performance of the fixed speed wind turbine system when subjected to consecutive three PCC voltage dips to 0.25 pu as shown in Fig. 4(a). The first fault is initiated at $t = 2.5$ s for a duration of 0.5 s, the second fault is initiated at $t = 4$ s for a duration of 0.75 s and the third fault is initiated at $t = 8$ s, for a duration of 0.8 s.

When the first fault is initiated, the generator voltage, V_g, falls to 0.185 pu as indicated in Fig. 4(b). At the fault clearance instant, $t = 3.5$ s, the machine draws a high inrush current, I_g, as illustrated in Fig. 4(c). Consequently, high reactive power, Q, is consumed as demonstrated in Fig. 4(d). Therefore, the generator terminal voltage is not recovered to its pre-fault value as depicted in Fig. 4(b). After a recovery period of about 0.6 s, the system is restored to its pre-fault state.

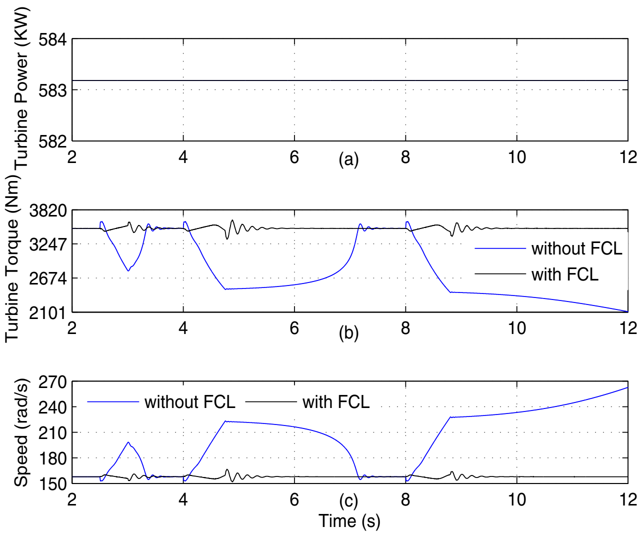

Fig. 7. Mechanical performance of the turbine with and without the proposed FCL.

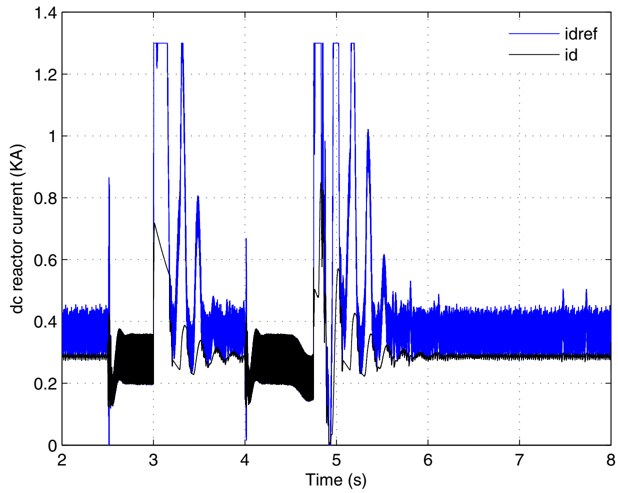

Fig. 8. The reference and actual signals for the dc current of the FCL during the first and second faults.

Similar dynamic performance is revealed during the second fault, except that the recovery period is increased due to the increased period of the fault. Increasing the fault period results in decreasing the generated active power, P_e, and hence the electromagnetic torque, T_e, as illustrated in Fig. 5(a) and (b), respectively. Since the mechanical torque, T_m, becomes higher than the electromagnetic torque, the generator shaft is accelerated to a higher speed than that of the first fault as indicated in Fig. 5(c). As a result, the operating point of the induction generator moves toward its critical stability limit at the moment of fault clearance. If the fault duration is increased, the induction generator may fail to recover if its operating point exceeds the stability limit where the electromagnetic torque becomes lower than that the turbine torque at the fault clearance. This case is demonstrated in the third fault where the generator continues acceleration after the fault clearance and the electromagnetic torque is diminished.

The wind turbine unit draws 4 MVAR from the grid during the recovery period as illustrated in Fig. 4(d). To reduce this value and to improve the dynamic performance of the wind turbine system, the proposed bridge-type FCL is applied and evaluated in the next subsection.

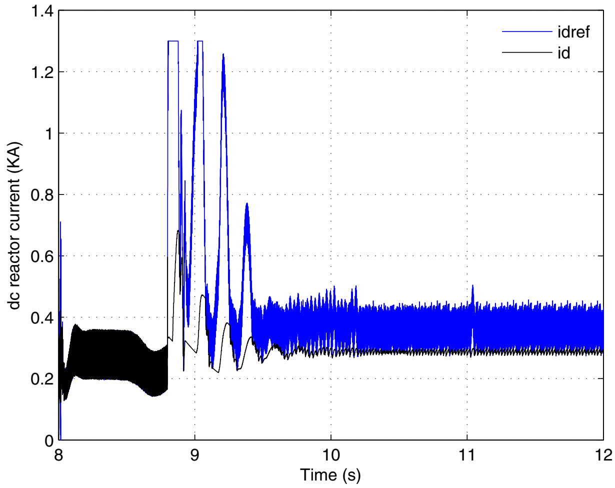

Fig. 9. The reference and actual signals for the dc current of the FCL during the third fault.

5.2. Fixed speed wind turbine with FCL

A bridge-type FCL with a discharging resistor is inserted in the system as shown in Fig. 2. The same faults of the previous case are simulated to evaluate the performance of the proposed control system of the FCL. Fig. 6 illustrates the dynamic performance of the system with the FCL. It is clear that the proposed FCL succeeds to regulate the generator voltage at 1 pu even during the periods of faults incidence and clearance as indicated in Fig. 6(b) with overvoltage less than 5%. As a result, the generator is not feeding the fault and its current is limited as shown in Fig. 6(c). Moreover, the problem of drawing heavy reactive power from the grid during fault clearance is solved as revealed from Fig. 6(d). The generated active power, electromagnetic torque, and the generator speed are illustrated in Fig. 6(e), (f), and (g), respectively. It is evident that the fluctuations of the generator power, torque, and speed are reduced compared to the uncompensated case. Furthermore, the proposed FCL stabilizes the WECS at the third fault. This action is expected because of limiting the generator current, limits the torque fluctuation and hence improves the stability margin as well as the FRT capability.

Fig. 7 evaluates the effect of the proposed FCL on the dynamic performance of the wind-turbine. Under the same wind condition, the mechanical power remains unchanged as indicated in Fig. 7(a). In the uncompensated case, the speed acceleration leads to torque fluctuation which is also function of the complex dynamics of the induction generator, especially during the recovery period. The proposed FCL succeeds to damp the mechanical vibration of the turbine during the grid faults and hence extends its life time.

Finally, the second cascaded loop which controls the dc current of the FCL is evaluated in Figs. 8 and 9. The reference and actual signals of the reactor current during the first and second faults are shown in Fig. 8. Fig. 9 illustrates the reactor current during the third fault. The actual current of the reactor tracks its reference signal during the fault and the normal conditions. The limit value of the dc current of the FCL is set at 1.3 kA. The dc current of the FCL approaches its limit value during the fault recovery period where the grid voltage is recovered, suddenly, with a phase angle that differs than that of the induction generator. However, the proposed control succeeds to limit the reactor current at the limit value during the fault clearance.

These results reveal that the proposed FCL enhance the dynamic performance of the WECS, improve the stability limit and FRT capability, and reduce the mechanical vibration of the turbine.

6. Conclusion

In this paper, the bridge-type FCL with a discharging resistor is utilized to protect a fixed speed WECS during the grid faults. The proposed control system regulates the terminal voltage of the generator and limits its current, simultaneously. The proposed FCL is simulated on PSCAD/EMTDC software package to evaluate the enhancements of the low voltage ride-through capability of fixed speed WECS turbine. The simulation results show that the proposed

FCL not only succeed in limiting the generator current during the fault, but also succeeds to damp the mechanical vibration of the turbine during the grid faults and hence extends its life time. Moreover, the proposed FCL improve the stability limit of the induction generator under grid fault conditions.

References

Abbott, S.B., Robinson, D.A., Perera, S., Darmann, F.A., Hawley, C.J., Beales, T.P., 2006. Simulation of HTS saturable core-type FCLs for MV distribution systems. IEEE Trans. Power Del. 21, 1013–1018.

Abramovitz, A., Smedley, K.M., 2012. Survey of solid-state fault current limiters. IEEE Trans. Power Electron. 27, 2770–2782.

Ali, M.H., 2012. Wind Energy Systems: Solutions for Power Quality and Stabilization. CRC Press, Boca Raton, FL, USA.

Ali, M.H., Wu, B., 2010. Comparison of stabilization methods for fixed-speed wind generator systems. IEEE Trans. Power Del. 25 (1), 323–331.

Awad, A.S.A., El Shatshat, R., Salama, M.M.A., EL-Fouly, T.H.M., 2014. Low voltage ride through capability enhancement of wind farms' generators: DVR versus STATCOM. In: IEEE PES General Meeting Conference and Exposition, 27–31 July, National Harbor, MD, USA.

Causebrook, A., Atkinson, D.J., Jack, A.G., 2007. Fault ride-through of large wind farms using series dynamic braking resistors. IEEE Trans. Power Syst. 22 (3), 966–975.

Chen, S., Li, P., Lehman, B., Ball, R., de Palma, J.-F., 2013. A new topology of bridge-type non-superconducting fault current limiter. In: IEEE Applied Power Electronics Conference and Exposition (APEC), 17–21 March, Long Beach, CA, USA.

Corzine, K.A., Ashton, R.W., 2012. A new Z-source DC circuit breaker. IEEE Trans. Power Electron. 27, 2796–2804.

Cvoric, D., de Haan, S.W.H., Ferreira, J.A., 2009. New saturable-core fault current limiter topology with reduced core size. In: IEEE International Power Electronics and Motion Control Conference (IPEMC), 17–20 May, Wuhan, China.

de Sousa, W.T.B., Polasek, A., Silva, F.A., Dias, R., Jurelo, A.R., de Andrade, R., 2012. Simulations and tests of MCP-BSCCO-2212 superconducting fault current limiters. IEEE Trans. Appl. Supercond. 22 (2), Article #: 5600106.

Firouzi, M., Gharehpetian, G.B., 2013. Improving fault ride-through of fixed-speed wind turbine by using bridge-type fault current limiter. IEEE Trans. Energy Conv. 28 (2), 361–369.

Hagh, M.T., Abapour, M., 2009. Non superconducting fault current limiter with controlling the magnitudes of fault currents. IEEE Trans. Power Electron. 24, 613–619.

Hussein, A.A., Ali, M.H., 2014. Comparison between DVR and SFCL for fault ride through capability improvement of fixed-speed wind generator. In: IEEE PES T&D Conference and Exposition, 14–17 April, Chicago, IL, USA.

Ise, T., Nguyen, N.H., Kumagai, S., 2001. Reduction of inductance and current rating of the coil and enhancement of fault current limiting capability of a rectifier type superconducting fault current limiter. IEEE Trans. Appl. Supercond. 11 (1), 1932–1935.

Leon, A.E., Farias, M.F., Battaiotto, P.E., Solsona, J.A., Valla, M.I., 2011. Control strategy of a DVR to improve stability in wind farms using squirrel-cage induction generators. IEEE Trans. Power Syst. 26 (3), 1609–1617.

Marei, M.I., El-Goharey, H.S.K., 2013. Dynamic performance analysis of a wind farm equipped with STATCOM. In: IEEE International Conference on Power Engineering, Energy and Electrical Drives (POWERENG), 13–17 May, Istanbul, Turkey.

Min, F.W., Li, Z.Y., Yu, L.Z., 2008. Novel bridge-type FCL based on self-turn off devices for three-phase power systems. IEEE Trans. Power Del. 23, 2068–2078.

Molinas, M., Suul, J.A., Undeland, T., 2008. Low voltage ride through of wind farms with cage generators: STATCOM versus SVC. IEEE Trans. Power Electron. 23 (3), 1104–1117.

Ramirez, D., Martinez, S., Platero, C.A., Blazquez, F., de Castro, R.M., 2011. Low voltage ride-through capability for wind generators based on dynamic voltage restorers. IEEE Trans. Energy Conv. 26 (1), 195–203.

Rashid, G., Ali, M.H., 2014. A modified bridge-type fault current limiter for fault ride-through capacity enhancement of fixed speed wind generator. IEEE Trans. Energy Conv. 29 (2), 527–534.

Ren, J., Hu, Y., Ji, Y., Liu, C., 2012. Low voltage ride-through control for fixed speed wind generators under grid unbalanced fault. In: IEEE Applied Power Electronics Conf. and Exposition (APEC), 5–9 February, Orlando, FL, USA.

Sheng, J., Jin, Z., Lin, B., Ying, L., Yao, L., Zhang, J., Li, Y., Hong, Z., 2012. Electrical–thermal coupled finite element model of high temperature superconductor for resistive type fault current limiter. IEEE Trans. Appl. Supercond. 22 (3), Article #: 5602004.

Tayyebifar, T., Shaker, M., Aghababaie, M., 2014. Performance comparison of STATCOM versus SVC to improve reactive power control in wind power based DFIG under short circuit fault. In: IEEE International Conference on Ecological Vehicles and Renewable Energies (EVER), 25–27 March, Monte-Carlo, Monaco.

Wiik, J.A., Fonstelien, O.J., Shimada, R., 2009a. A MERS type series FACTS controller for low voltage ride through of induction generators in wind farms. In: European Conference on Power Electronics and Applications (EPE), 8–10 September, Barcelona, Spain.

Wiik, J.A., Wijaya, F.D., Shimada, R., 2009b. Characteristics of the magnetic energy recovery switch (MERS) as a series FACTS controller. IEEE Trans. Power Del. 24 (2), 828–836.